



## Discovery and initial SAR of pyrimidin-4-yl-1H-imidazole derivatives with antiproliferative activity against melanoma cell lines

Junghun Lee, Hwan Kim, Hana Yu, Jae Yoon Chung, Chang-Hyun Oh, Kyung Ho Yoo, Taebo Sim, Jung-Mi Hah\*

Life/Health Division, Korea Institute of Science and Technology, PO Box 131, Cheongryang, Seoul 130-650, Republic of Korea

### ARTICLE INFO

#### Article history:

Received 8 December 2009  
Revised 12 January 2010  
Accepted 13 January 2010  
Available online 21 January 2010

#### Keywords:

Pyrimidin-4-yl-1H-imidazol-2-yl derivatives  
Antiproliferative activity  
Melanoma cell line  
BRAF  
CRF  
Selectivity

### ABSTRACT

The synthesis of a novel series of pyrimidin-4-yl-1H-imidazol-2-yl derivatives **7**, **8**, **9** and their antiproliferative activities against A375P human melanoma cell line and WM3629 cell line were described. Most compounds showed superior antiproliferative activities compared to Sorafenib, the well-known RAF inhibitor. Among them, **7a** exhibited potent activities on both cell lines ( $IC_{50}$  = 0.62 and 4.49  $\mu$ M, respectively) and turned out to be a selective and potent CRAF inhibitor.

© 2010 Elsevier Ltd. All rights reserved.

Skin cancer is the most common form of cancer in the United States.<sup>1</sup> Although melanoma is the least common type of skin cancer; it is the most serious form of the disease. Melanoma occurs in *melanocytes*, a type of cell in the skin that produces the pigment that gives skin its natural color. Melanoma begins when melanocytes become malignant, which can occur on any skin surface. Once melanoma cells migrates to other organs, it is notoriously refractory to current treatment regimens, which induce responses in only 10–20% of patients.<sup>2,3</sup>

In the vast majority of melanomas, the mitogen-activated protein kinase (MAPK; RAS-RAF-MEK-ERK) and the phosphoinositide 3-kinase-AKT pathways are up-regulated,<sup>4,5</sup> and alteration of signaling through both pathways plays a major role in melanoma progression.

Especially, the discovery of activating V600E BRAF mutations in approximately 50% of melanomas has raised the expectations for targeted therapy.<sup>6,7</sup> As a result, the pharmacological targeting of BRAF/MAPK signaling in melanoma is now being intensively studied in both the clinical and preclinical settings.<sup>8</sup>

However, there is now a growing consensus being made that there are significant ratio of melanomas (>33%) that do not contain BRAF V600E mutations that may involve alternative therapeutic targets<sup>9</sup>, and one of which is closely related CRAF (or Raf-1).<sup>10,11</sup>

Previous generations of RAF inhibitors include pyrazole compounds from Pfizer,<sup>12</sup> SB-590885,<sup>13</sup> PLX4720,<sup>14</sup> sorafenib<sup>15</sup> (Fig. 1: Launched for RCC), and PLX4032 (Phase II for melanoma and colorectal cancer). The bi-aryl urea sorafenib is a potent inhibitor of preactivated CRAF and BRAF as well as oncogenically activated BRAF kinases (V600E BRAF:  $IC_{50}$  = 43 nM).

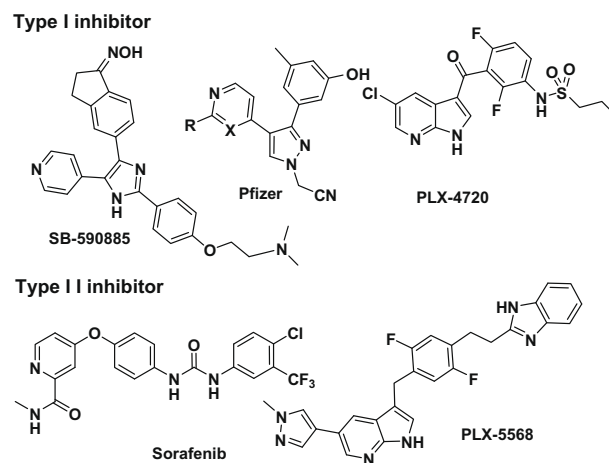
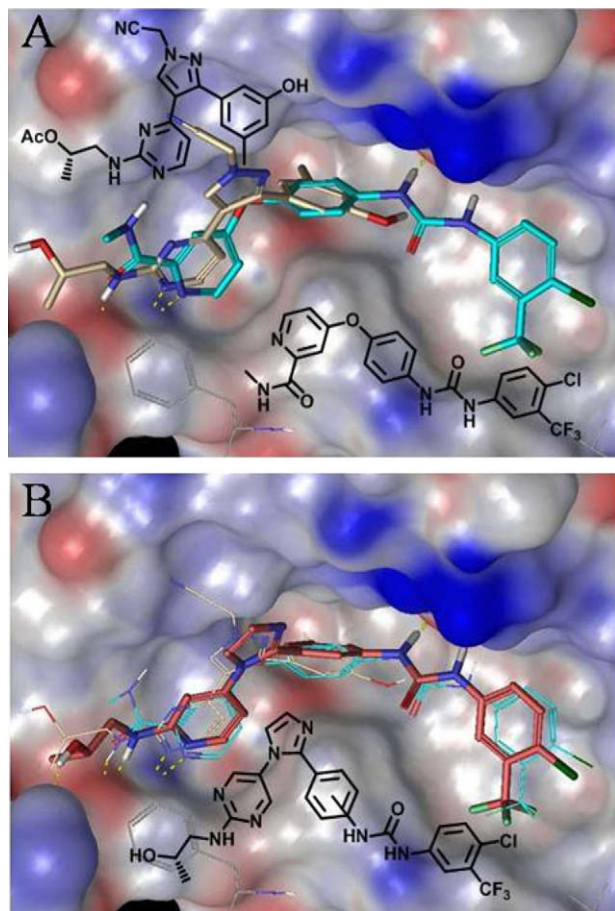


Figure 1. Structure of known V600E RAF inhibitors.

\* Corresponding author. Tel.: +82 2 958 6438; fax: +82 2 958 5189.  
E-mail address: jhah@kist.re.kr (J.-M. Hah).



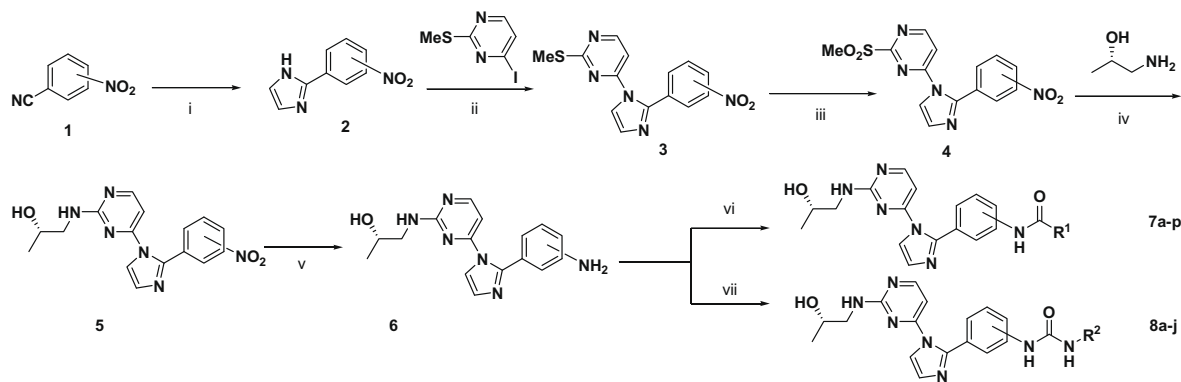
**Figure 2.** (A) Crystal structure of Sorafenib (cyan) and a docking structure of Pfizer scaffold (yellow) in V600E BRAF (1UWH); (B) Docking structure of a novel chimera scaffold (red; Glide in Schrödinger package).

Crystal structure of V600E BRAF kinase domains in complex with sorafenib showed that the inhibitor held the activation segment in an inactive conformation, preventing ATP binding and subsequent kinase reaction. Although sorafenib failed to show therapeutic activity in melanoma, the binding feature is interesting enough to prompt us to design a novel scaffold for RAF inhibitor, especially, it occupies the unique secondary hydrophobic pocket in inactive conformation of kinase domain, namely Type II inhibitor.<sup>16</sup> However, there are many numbers of Type I inhibitors for RAF has been also known having a much better potency (see Fig. 2).

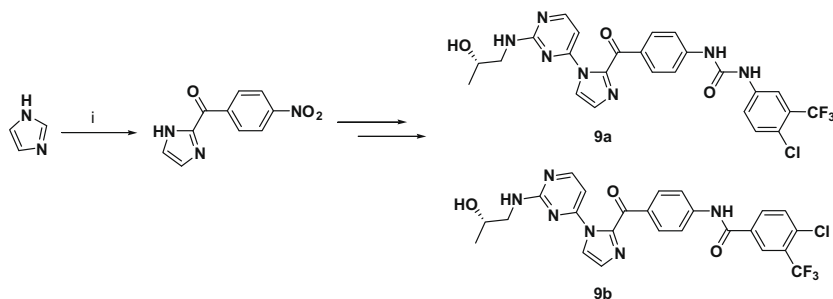
Here we could come up with a novel chimera scaffold for RAF inhibitors, which possibly have a potent hinge binder and take advantage of secondary hydrophobic pocket as well.<sup>16</sup> The structure of this series comprises 1-pyrimidinyl imidazole part as a hinge binder, the middle phenyl ring moiety and various aromatic tail part connected by amide or urea linkage.

We designed the scaffold to aim the middle phenyl ring moiety to be orthogonal to the imidazole ring for the effective conformation for hydrophobic pocket. To get more potent inhibitor, we tried to modify the structures by (a) introducing the various direction of connectivity in the middle phenyl moiety (*m*-, *p*-) and (b) changing the aromatic tail part to understand the depth and shape of secondary hydrophobic pocket in inactive conformation.

The general synthesis of pyrimidin-4-yl-1*H*-imidazol-2-yl derivatives is shown in Scheme 1. The nitrophenyl imidazole moiety was synthesized from 2,2-dimethoxyethanamine and imidate in situ, which was formed from 3- or 4-nitrobenzonitrile and methoxide under alkaline catalysis in one pot process based on the literature.<sup>17</sup> Then nitrophenyl imidazole was coupled with 4-iodo-2-(methylthio)pyrimidine in a modified Buchwald condition. Further, methylthio group was oxidized using *m*CPBA to methyl sulfoxide and substituted with (*S*)-1-aminopropan-2-ol. Without protection on hydroxy group, nitro group on phenyl ring was reduced to give amine and coupled with various aromatic acids under EDCI/HOBt conditions or directly aromatic isocyanate to give amide (**7a–7p**) or urea (**8a–8j**) analogues.

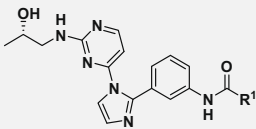
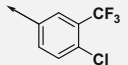
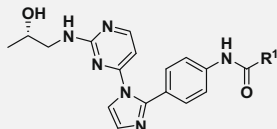
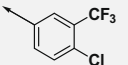
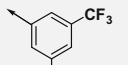
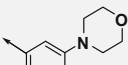
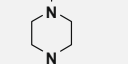
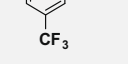
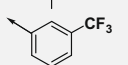
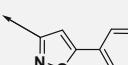
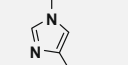
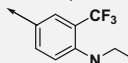
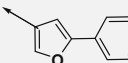
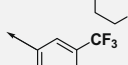
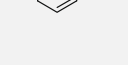
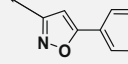


**Scheme 1.** Reagents and conditions: (i) 30% NaOMe, MeOH; 2,2-dimethoxyethanamine, AcOH 50 °C; 6 N HCl in H<sub>2</sub>O–MeOH; (ii) Pd<sub>2</sub>(dba)<sub>3</sub>, BINAP, NaOtBu, toluene, 150 °C, 3 h; (iii) *m*-CPBA, CH<sub>2</sub>Cl<sub>2</sub>, rt, 8 h; (iv) THF, 60 °C, 5 h; (v) 10% Pd/C, MeOH, rt, 6 h; (vi) R<sup>1</sup>CO<sub>2</sub>H, EDCI, TEA, HOBt, DMF; (vii) R<sup>2</sup>NCO, THF, rt, 12 h.



**Scheme 2.** Reagents and conditions: (i) 4-nitrobenzoyl chloride, TEA, pyridine 0 °C to rt.

**Table 1**  
Antiproliferative activity of pyrimidin-4-yl-1H-imidazol-2-yl derivatives and pyrimidin-4-yl-1H-imidazole-2-carbonyl derivatives with Sorafenib as reference compound

Structure	No.	R	GI <sub>50</sub> (μM)		Structure	No.	R	GI <sub>50</sub> (μM)	
			WM3629	A375P				WM3629	A375P
	7a <sup>22</sup>		0.62	4.49		7j		>100	79.2
	7b		9.13	10.4		7k		2.25	35.6
	7c		3.49	6.72		7l		>100	>100
	7d		7.37	28.3		7m		>100	8.05 <sup>a</sup>
	7e		NA	NA		7n		>100	2.23
	7f		>100	164 <sup>a</sup>		7o		>100	139
	7g		NA	NA		7p		>100	>100
	7h		22.3	>100					
	7i		13.8	>100					

(continued on next page)

Table 1 (continued)

Structure	No.	R	GI <sub>50</sub> (μM)		Structure	No.	R	GI <sub>50</sub> (μM)	
			WM3629	A375P				WM3629	A375P
	8a		>100	58.2		8g		4.43	10.1
	8b <sup>22</sup>		0.65	5.93		8h		2.45	17.8
	8c		>100	85.8		8i		12.9	7.19
	8d		7.86	19.2		8j		4.99	3.19
	8e		3.28	34.6		9a		1.37	2.51
	8f		4.54	19.4		9b		3.51	9.29
Sorafenib								0.78	5.58

<sup>a</sup> Maximum potency showed less than 60% of total growth.

To investigate an optimal location of hydrophobic tail and urea- or amide-linkage, we attempted extra carbonyl insertion between imidazole and phenyl ring and synthesized two compounds with pyrimidin-4-yl-1*H*-imidazole-2-carbonyl derivatives (**9a**, **9b**), which is shown in Scheme 2. The imidazole and nitrobenzoyl chloride was coupled in basic condition to form core structure and the rest of reactions were completed as the same as in Scheme 1.

We examined the antiproliferative activity of these pyrimidinyl imidazole derivatives in two melanoma cell lines (human A375P and WM3629).<sup>18,19</sup> Unlike well-known A375P melanoma cell lines, the WM3629 cell lines were used since it could represent non-V600E mutated melanoma cell lines (>33%). Instead of V600E mutation, this cell line depends on low activity mutant BRAF (D594G) and more importantly, CRAF for the proliferation.<sup>9,20</sup> We chose sorafenib as the reference standard because it has been extensively studied for melanoma and also for CRAF inhibition.

The antiproliferative activity of pyrimidin-4-yl-1*H*-imidazole-2-yl derivatives and pyrimidin-4-yl-1*H*-imidazole-2-carbonyl derivatives are shown in Table 1. Generally, they show a variety of potency range depending on the substitution pattern of middle phenyl ring and more importantly, on the tail group (R) implying that the activity is more sensitive to the secondary hydrophobic pocket (see Table 2).

When the middle phenyl ring has *m*- orientation, the amide compounds with relatively short tail possessed good potency, especially **7a** showed the best potency toward WM3629 cell line (GI<sub>50</sub> = 620 nM) in this series and it was better than the reference sorafenib. But when the tail has been extended to bicyclic structure, the smaller aromatic ring was preferred as second ring and the substitution pattern was favored in 1, 3, 5-position (**7c** > **7b**, **7d**). The five-membered aromatic ring-extended bicyclic tail did not improve the potency at all (**7f**–**7i**).

In case of *m*-oriented urea derivatives (**8a**–**8f**), the compound with less bulky substitutions on the phenyl ring tail showed relatively better potency on both cell lines. It was quite surprising to see that the small difference in substitution on 3-position of

Table 2

Percentages of enzymatic inhibitions exerted by **7a** (10 μM) on selected 30 Protein Kinases

Kinase	% Inhibition
AKT1	5.1
ALK	0.8
c-Src	≤0
CDK1/cyclinB	21
CDK2/cyclinE	≤0
CDK5/p25	2.4
CHK1	5.9
DMPK	7.6
DNA-PK	9.4
EGFR/ERBB1	1.7
ERK2/MAPK1/P42MAPK	10
FAK/PTK2Axl(h)	0
Flt3(h)	82
GSK3b	14
IGF-1R	3.6
JAK3	0.21
JNK1/MAPK8	≤0
LYN/LYN A	21
MEK1	≤0
mTOR/FRAP1	1.5
P38α/MAPK14	89
p70S6K/RPS6KB1	17
PAK4	≤0
PKA	6.8
PKCa	1.1
CRAF	99
RON/MST1R	5.0
ROS/ROS1	0.19
SYK	13
TRKB/NTRK2	≤0

benzoic acid tail made a big difference in their cellular activity (**8a**, **8c** vs **8b**).

Overall the compounds with middle phenyl ring of *p*-substitution (**7j–7p**, **8g–8j**) showed mild potency toward both cell lines. Considering that the ratio of  $GI_{50}$  for A375P/WM3629 could be used as the rough index for selectivity of BRAF/CRAF, compounds with middle phenyl ring of *m*-substitution and sorafenib showed 5–10-fold selective for WM3629 over A375P. However, it seems that the compounds with middle phenyl ring of *p*-substitution show less selectivity or even a reverse trend, especially in case of **8i** and **8j**.

In case of pyrimidin-4-yl-1*H*-imidazole-2-carbonyl derivatives (**9**), the most potent compound on A375P cell lines in this series (**9a**) was found. As we expected in docking experiment (data not shown), the amide derivative was better than the corresponding urea (**9b**).

Generally, the activity toward WM3629 cell line showed higher than A375P, but there are several compounds (**7j**, **7m**, **7n**, **8a**, **8c** and data not presented) which show the reverse trend, and that could be a valuable information for designing a selective each iso-type of RAF inhibitor.

We further tried kinase panel screening of the compound **7a** over 30 different kinases at a single dose concentration of  $10\ \mu\text{M}^{21}$  (done in duplicate) and it was revealed that the compound was indeed a selective CRAF inhibitor with a superb selectivity profile. While this compound has inhibitory activity of 99% on CRAF at this concentration, the inhibition activity was below than 20% in most other kinase tested except p38 $\alpha$ , and Flt3.

In conclusion, a series of pyrimidin-4-yl-1*H*-imidazol-2-yl derivatives based on the structural features of sorafenib showed potent antiproliferative activities against both A375P and WM3629 human melanoma cell lines. Especially, in our series, **7a**, **7c**, **8j**, **9a** exhibited competitive activities on A375P cell line and **7a**, **8b** showed superior activities on WM3629 cell line compared to sorafenib. These results suggest that pyrimidin-4-yl-1*H*-imidazol-2-yl scaffold possesses a possibility as a therapeutic agent for melanoma and all these findings will be combined for further development of potent and selective RAF inhibitors.

## Acknowledgments

This research was supported by Korea Institute of Science and Technology (KIST) and Basic Science Research Program through the National Research Foundation of Korea (NRF) funded by the Ministry of Education, Science and Technology (2009-0087992; J.M.H.). We also thank Dr. Merlyn lab at Wistar Institute for the kind supply of WM3629 cell line.

## References and notes

- Jemal, A.; Siegel, R.; Ward, E. *CA Cancer J. Clin.* **2008**, *58*, 71.
- Nashan, D.; Muller, M. L.; Grabbe, S.; Wustlich, S.; Enk, A. J. *Eur. Acad. Derm. Venol.* **2007**, *21*, 1305.
- Carlson, J. A.; Ross, J. S.; Slominski, A.; Linette, G.; Mysliborski, J.; Hill, J.; Mihm, M., Jr. *J. Am. Acad. Dermatol.* **2005**, *52*, 743.
- Smalley, K. S. *Int. J. Cancer* **2003**, *104*, 527.
- Dhawan, P.; Singh, A. B.; Ellis, D. L.; Richmond, A. *Cancer Res.* **2002**, *62*, 7335.
- Davies, H.; Bignell, G. R.; Cox, C.; Stephens, P.; Edkins, S.; Clegg, S. *Nature* **2002**, *417*, 949.
- Houben, R.; Vetter-Kauczok, C. S.; Ortmann, S.; Rapp, U. R.; Broecker, E. B.; Becker, J. C. *J. Invest. Dermatol.* **2008**, *128*, 2003.
- Eisen, T.; Ahmad, T.; Flaherty, K. T.; Gore, M.; Kaye, S.; Marais, R. *Br. J. Cancer* **2006**, *95*, 581.
- Smalley, K. S. M.; Xiao, M.; Villaneva, J.; Nguyen, T. K.; Flaherty, K. T.; Letrero, R.; Van Belle, P.; Elder, D. E.; Wang, Y.; Nathanson, K. L.; Herlyn, M. *Oncogene* **2009**, *28*, 85.
- Jilaveanu, L.; Zito, C. R.; Aziz, S. A.; Conrad, P. J.; Schmitz, J. C.; Szno, M.; Camp, R. L.; Rimm, D. L.; Kluger, H. M. *Clin. Cancer Res.* **2009**, *15*, 5704.
- Dumaz, N.; Hayward, R.; Martin, J.; Ogilvie, L.; Hedley, D.; Curtin, J. A.; Bastian, B. C.; Springer, C.; Marais, R. *Cancer Res.* **2006**, *66*, 9483.
- Bennett, M. J. et al. WO2007105058A2.
- King, A. J.; Patrick, D. R.; Batorsky, R. S.; Ho, M. L.; Do, H. T.; Zhang, S. Y.; Kumar, R.; Huang, P. S., et al. *Cancer Res.* **2006**, *23*, 11100.
- Tsai, J.; Lee, J. T.; Wang, W.; Zhang, J.; Cho, H.; Bollag, G., et al. *Proc. Natl. Acad. Sci.* **2008**, *105*, 3041.
- Wilhelm, S. M.; Adnane, L.; Newell, P.; Villanueva, A.; Llovet, J. M.; Lynch, M. *Mol. Cancer Ther.* **2008**, *7*, 3129.
- Liu, Y.; Gray, N. S. *Nat. Chem. Biol.* **2006**, *2*, 358.
- Voss, M. E.; Beer, C. M.; Mitchell, S. A.; Blmgren, P. A.; Zhichkin, P. E. *Tetrahedron* **2008**, *64*, 645.
- A375P cells were purchased from American Type Culture Collection (ATCC, Rockville, MD, US) and maintained in DMEM medium (Welgene, Daegu, Korea) supplemented with 10% FBS (Welgene) and 1% penicillin/streptomycin (Welgene) in a humidified atmosphere with 5% CO<sub>2</sub> at 37 °C. A375P cells were taken from culture substrate with 0.05% trypsin-0.02% EDTA and plated at a density of  $5 \times 10^3$  cells/well in 96 well plates and then incubated at 37 °C for 24 h in a humidified atmosphere with 5% CO<sub>2</sub> prior to treatment of various concentration (three-fold serial dilution, 12 points) of test compounds. The A375P cell viability was assessed by the conventional 3-(4,5-dimethylthiazol-2-yl)-2,5-diphenyltetrazolium bromide (MTT) reduction assay. MTT assays were carried out with CellTiter 96<sup>®</sup> (Promega) according to the manufacturer's instructions. The absorbance at 590 nm was recorded using EnVision 2103 (Perkin Elmer; Boston, MA, US). The IC<sub>50</sub> was calculated using GraphPad Prism 4.0 software.
- WM3629 cell line was supplied from Dr. Merlyn lab at Wistar Institute (Philadelphia, PA, US) and maintained in Tu2% medium according to the literature 9. The procedure for  $GI_{50}$  determination (MTT assay) was the same as in A375P cell line.
- Montagut, C.; Sharma, S. V.; Shioda, T.; McDermott, U.; Ulman, M.; Ulkus, L. E.; Dias-Santagata, D.; Stubbs, H.; Lee, D. Y.; Singh, A.; Drew, L.; Haber, D. A.; Settleman, J. *Cancer Res.* **2008**, *68*, 4853.
- We used Reaction Biology Corp. Kinase HotSpot<sup>SM</sup> service ([www.reactionbiology.com](http://www.reactionbiology.com)) for screening of **7a**.
- Selected data. Compound **7a**: <sup>1</sup>H NMR (400 MHz, DMSO-*d*<sub>6</sub>)  $\delta$  10.60 (1H, s), 8.37 (1H, s), 8.30 (1H, d, *J* = 5.24 Hz), 8.24 (1H, dd, *J* = 1.94 Hz, *J* = 1.83 Hz), 7.94 (1H, s), 7.92 (1H, s), 7.84 (1H, d, *J* = 8.79 Hz), 7.73 (1H, br s), 7.39 (1H, t, *J* = 8.02 Hz), 7.30 (1H, br s), 7.21 (1H, s), 7.09 (1H, d, *J* = 6.72 Hz), 4.50 (1H, br s), 3.77 (1H, m), 3.61 (1H, m), 2.89 (2H, m), 1.26 (3H, d, *J* = 8.13 Hz); MS *m/z* 533 (M+H)<sup>+</sup>. Compound **8b**: <sup>1</sup>H NMR (400 MHz, CDCl<sub>3</sub>)  $\delta$  8.20 (1H, s), 8.16 (1H, s), 7.55–7.51 (2H, m), 7.27 (1H, s), 7.23–7.18 (3H, m), 7.13–7.07 (3H, m), 6.91 (1H, *J* = 7.13 Hz), 6.22 (1H, s), 5.61–5.60 (1H, br s), 4.98–4.96 (1H, br s), 3.48–3.47 (1H, m), 3.18–3.00 (2H, m), 1.27 (3H, t, *J* = 9.24 Hz); MS *m/z* 499 (M+H)<sup>+</sup>.